Inhibition of Intestinal Polyposis with Reduced Angiogenesis in *Apc*$^{Min/+}$ Mice Due to Decreases in c-Myc Expression

Krishna Yekkala and Troy A. Baudino

Department of Cell and Developmental Biology and Anatomy, University of South Carolina School of Medicine, Columbia, South Carolina

Abstract

The c-*myc* oncogene plays an important role in tumorigenesis and is frequently deregulated in many human cancers, including gastrointestinal cancers. In humans, mutations of the adenomatous polyposis coli (*Apc*) tumor suppressor gene occur in most colorectal cancers. Mutation of *Apc* leads to stabilization of β-catenin and increases in β-catenin target gene expression (c-*myc* and *cyclin D1*), whose precise functional significance has not been examined using genetic approaches. *Apc*$^{Min/+}$ mice are a model of familial adenomatous polyposis and are heterozygous for an Apc truncation mutation. We have developed a model for examining the role of c-Myc in Apc-mediated tumorigenesis. We crossed c-*myc*$^{+/-}$ mice to *Apc*$^{Min/+}$ to generate *Apc*$^{Min/+}$ c-*myc*$^{+/-}$ animals. The compound *Apc*$^{Min/+}$ c-*myc*$^{+/-}$ mice were used to evaluate the effect of c-*myc* haploinsufficiency on the *Apc*$^{Min/+}$ phenotype. We observed a significant reduction in tumor numbers in the small intestine of *Apc*$^{Min/+}$ c-*myc*$^{+/-}$ mice compared with control *Apc*$^{Min/+}$ c-*myc*$^{+/+}$ mice. In addition, we observed one to three polyps per colon in *Apc*$^{Min/+}$ c-*myc*$^{+/+}$ mice, whereas only two lesions were observed in the colons of *Apc*$^{Min/+}$ mice that were haploinsufficient for c-*myc*. Moreover, reduction in c-*myc* levels resulted in a significant increase in the survival of these animals. Finally, we observed marked decreases in *vascular endothelial growth factor, EphA2*, and *ephrin-B2* expression as well as marked decreases in angiogenesis in intestinal polyps in *Apc*$^{Min/+}$ c-*myc*$^{+/-}$ mice. This study shows that c-Myc is critical for Apc-dependent intestinal tumorigenesis in mice and provides a potential therapeutic target in the treatment of colorectal cancer. (Mol Cancer Res 2007;5(12):1296–303)

Received 5/24/07; revised 7/31/07; accepted 8/7/07.
Grant support: NIH grant RR017698.
The costs of publication of this article were defrayed in part by the payment of page charges. This article must therefore be hereby marked *advertisement* in accordance with 18 U.S.C. Section 1734 solely to indicate this fact.
Requests for reprints: Troy A. Baudino, Department of Cell and Developmental Biology and Anatomy, University of South Carolina School of Medicine, 6439 Garners Ferry Road, Building #1, C-57, Columbia, SC 29209. Phone: 803-733-1562; Fax: 803-733-1533. E-mail: tbaudino@med.sc.edu

doi:10.1158/1541-7786.MCR-07-0232

Introduction

Mutation and inactivation of the adenomatous polyposis coli (*Apc*) tumor suppressor gene is an early event in the development of colorectal cancer (1). Inactivation of Apc occurs in ~80% of adenomatous polyps and it is also responsible for the genetic disorder familial adenomatous polyposis, which leads to the formation of adenomatous polyps in the small and large intestine that results in colon cancer (2-4). It has been shown that the major function of Apc is to degrade cytosolic levels of β-catenin, thus preventing formation of the β-catenin/T-cell factor-4 complex and effectively blocking β-catenin/T-cell factor-4–meditated transcription (5). Interestingly, mice lacking T-cell factor-4 display no proliferating cells in their intestinal crypts, suggesting that this signaling pathway is essential for intestinal proliferation (6). Multiple downstream targets for β-catenin have been identified, including *cyclin D1* and c-*myc*, two factors that are critical for cell cycle traverse and other biological processes (7, 8). Indeed, previous studies have shown that c-*myc* expression is repressed by Apc and is increased by overexpression of β-catenin in human colon cancer cells (7, 9). Although these two β-catenin target genes are likely to be important for colorectal tumorigenesis, the exact functional significance of these targets has yet to be clearly defined. The *c-myc* gene encodes a transcription factor with a basic helix-loop-helix leucine zipper domain that mediates heterodimerization with its obligate DNA-binding partner Max. This basic helix-loop-helix leucine zipper domain is also essential for direct DNA binding. Myc activates or represses the transcription of a wide array of target genes that elicit a variety of biological responses, including cell growth, proliferation, differentiation, metabolism, and apoptosis (10-12). In addition, the role of Myc during development has been examined in several tissues, including the gastrointestinal tract (13). Previous data from the Trumpp laboratory showed that c-Myc is essential for intestinal crypt formation but is dispensable for maintenance and homeostasis of the adult intestinal epithelium (13). These data were surprising because c-Myc is generally essential for cell cycle traverse. Thus, the role of c-Myc during development and homeostasis of the intestine remains to be discovered. Additionally, c-Myc has also been shown to modulate the expression of various angiogenic factors, including vascular endothelial growth factor (VEGF; refs. 14-16). Moreover, c-Myc has been shown to down-regulate antiangiogenic factors, such as *thrombospondin-1* (14, 17, 18). The importance of Myc in cancer is evident by its increased expression in many human cancers, including colon, breast, prostate, and lung (19). Furthermore, Myc overexpression in various cell types in mice

induces tumors that display increased proliferation, delayed differentiation, and increased angiogenesis (16, 20). Indeed, c-Myc levels are increased in the tumors of $Apc^{Min/+}$ mice and deletion of c-*myc* results in reduced tumorigenesis due to increases in apoptosis (21). However, these previous studies from the Gerner and Trumpp laboratories did not examine other biological processes in which Myc is involved, specifically angiogenesis. Therefore, because c-Myc expression is increased in the $Apc^{Min/+}$ mouse model of familial adenomatous polyposis, it is possible that this leads to increases in c-Myc target gene expression and promotes progression through the adenoma-carcinoma sequence and subsequent metastasis. Thus, the aim of the present study was to evaluate the role of c-Myc on tumorigenesis in the $Apc^{Min/+}$ murine model.

Results

c-myc Haploinsufficiency Increases the Survival of $Apc^{Min/+}$ Mice and Greatly Decreases Tumor Incidence and Size

It has been previously shown that *c-myc* is a β-catenin target gene, and in $Apc^{Min/+}$ mice, the levels of c-*myc* are significantly increased when compared with wild-type (WT) animals (7, 9). Moreover, it has been previously shown that complete deletion of c-*myc* in the intestinal tract does not perturb normal intestinal homeostasis but does disrupt the formation of intestinal crypts (13). In addition, recent studies from Sansom et al. (22) show that c-*myc* deletion blocks tumorigenesis in *Apc*-deficient mice in the small intestine, suggesting that Myc is a critical mediator of neoplasia following *Apc* loss. Furthermore, recent studies from the Gerner laboratory showed that c-*myc* loss (2-fold reduction in protein) resulted in reduced tumorigenesis in $Apc^{Min/+}$ mice due to increased levels of apoptosis (21). Thus, to further investigate the role of c-Myc in Apc-mediated tumorigenesis, we crossed $Apc^{Min/+}$ mice with c-$myc^{+/-}$ animals to generate $Apc^{Min/+}$ c-$myc^{+/-}$ mice. We then followed the life span of these animals, with mice being humanely sacrificed when moribund. Mice that were WT for c-*myc* and $Apc^{Min/+}$ had a median life span of 169 days, whereas animals that were heterozygous for c-*myc* and $Apc^{Min/+}$ lived an average of 291 days (Fig. 1). Amazingly, many of the animals that were $Apc^{Min/+}$ c-$myc^{+/-}$ were still alive at 1 year of age (Fig. 1).

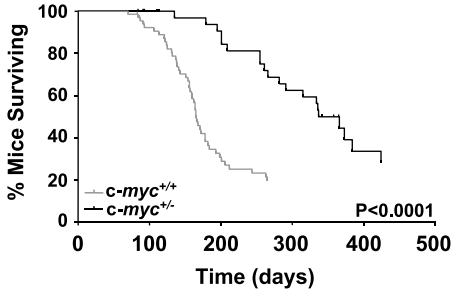

FIGURE 1. Survival curve of $Apc^{Min/+}$ mice that are WT or haploinsufficient for c-*myc*. Loss of a single allele of c-*myc* results in a dramatic increase in the life span of $Apc^{Min/+}$ animals. $Apc^{Min/+}$ mice that are WT for c-*myc* (*gray*) or heterozygous for c-*myc* (*black*) are shown. Mice that were WT for c-*myc* and $Apc^{Min/+}$ had a median life span of 169 d (n = 65), whereas animals that were heterozygous for c-*myc* had a median life span of 291 d (n = 37).

Having observed the dramatic increase in survival of $Apc^{Min/+}$ c-$myc^{+/-}$ animals, we next examined the intestines of age-matched (12 weeks) animals to determine if the observed increase in survival was due to a decrease in polyp number and/or size or if there was another underlying cause. Indeed, in 12-week-old age-matched animals, we observed a significant reduction in the total number of polyps, as well as marked decreases in polyp numbers of various sizes, with the largest decreases observed in polyps that were >2.0 mm in size (Fig. 2A). In addition, similar reductions in polyp numbers were observed in moribund animals (Fig. 2B). Moreover, whereas most of the $Apc^{Min/+}$ c-$myc^{+/+}$ mice displayed between one and three colonic polyps with an 80% incidence rate, only two of the c-$myc^{+/-}$ animals displayed a colonic polyp (10% incidence rate; Fig. 2C). Furthermore, gross analyses of whole intestine or H&E staining of intestinal sections further showed the dramatic reduction in polyp number and size with the loss of only a single c-*myc* allele (Fig. 2D and E) Taken together, these data suggest that c-Myc is playing a critical role in the initial development and growth of these intestinal and colonic polyps and that by simply reducing c-Myc levels we observe a marked reduction in polyp number and a dramatic increase in survival.

Cell Proliferation Is Reduced in the Intestinal Polyps of $Apc^{Min/+}$ c-$myc^{+/-}$ Mice

Myc has been shown to play a critical role in cell cycle traverse and apoptosis during development as well as in cancer. Indeed, previous studies from Ignatenko et al. (21) showed that c-*myc* loss in $Apc^{Min/+}$ mice resulted in marked increases in apoptosis. However, recent studies from Alan Clarke's laboratory have shown that Myc deficiency shows remarkably little effect on cell proliferation but does cause a block in apoptosis in the small intestine in the absence of *Apc* (22). Nonetheless, having observed a dramatic reduction in polyp size and number in animals that were heterozygous for c-*myc*, we chose to examine the effect of c-*myc* reduction on cell proliferation in the intestinal polyps of $Apc^{Min/+}$ c-$myc^{+/-}$ mice. Therefore, we isolated intestines from 12-week-old age-matched animals and examined intestinal polyps for the presence of phospho-histone H3–positive cells (Fig. 3A). Computational analyses of immunofluorescent images showing staining for nuclei (4′,6-diamidino-2-phenylindole, blue) or phospho-histone H3 (red) showed a significant difference in levels of cell proliferation in intestinal polyps present in $Apc^{Min/+}$ c-$myc^{+/+}$ mice when compared with animals that were $Apc^{Min/+}$ c-$myc^{+/-}$ (Fig. 3A and B).

Apoptosis Is Increased in the Intestinal Polyps of $Apc^{Min/+}$ c-$myc^{+/-}$ but not in Normal Intestinal Crypts

To examine apoptotic levels, we did terminal deoxynucleotidyl transferase–mediated dUTP nick end labeling (TUNEL) analyses on intestinal sections from $Apc^{Min/+}$ c-$myc^{+/+}$ and $Apc^{Min/+}$ c-$myc^{+/-}$ mice. Not surprisingly, we did not see any differences in the levels of apoptosis in the normal intestinal crypts of $Apc^{Min/+}$ mice that are WT (12.8%) or haploinsufficient for c-*myc* (12.7%; Fig. 4A-C). These data are similar to those observed in recent studies examining c-*myc* loss in the small intestine (13) as well as our previous studies examining

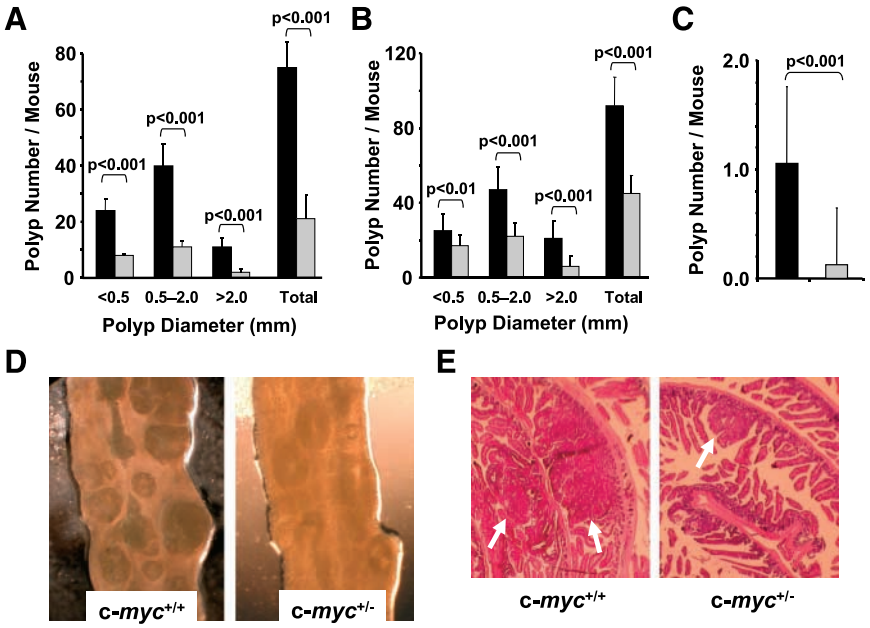

FIGURE 2. Intestinal and colonic polyp numbers are reduced in $Apc^{Min/+}$ c-$myc^{+/-}$ animals. **A.** Intestinal polyps were counted according to size in 12-wk-old age-matched animals that were either WT (*black columns*) or heterozygous (*gray columns*) for c-*myc* (n = 10 for each group). We observed a 67% reduction in polyps <0.5 mm in size, a 75% reduction in polyps 0.5 to 2.0 mm in size, and a 90% reduction in polyps >2.0 mm in size in c-$myc^{+/-}$ animals. **B.** Intestinal polyps were counted according to size in moribund animals that were either WT (*black columns*; n = 29) or heterozygous (*gray columns*; n = 20) for c-*myc*. Again, notice the marked reduction in the number of polyps present in c-$myc^{+/-}$ animals. **C.** Total numbers of colonic polyps were counted in moribund animals. There was a >90% reduction in the number of colonic polyps per mouse in animals that were heterozygous for c-*myc*. In fact, only two c-$myc^{+/-}$ animals (n = 20) displayed any colonic polyps. **D.** Representative images of intestines isolated from age-matched (12 wk) $Apc^{Min/+}$ mice that were either WT (*left*) or heterozygous (*right*) for c-*myc*. Notice the marked decrease in the number and size of polyps present in c-$myc^{+/-}$ animals. **E.** Representative H&E-stained sections for $Apc^{Min/+}$ mice that were WT (*left*) or heterozygous (*right*) for c-*myc*. Notice the decrease in polyp size (*white arrows*) in c-$myc^{+/-}$ animals.

c-*myc* loss in the whole E9.5 murine embryo (14). However, the number of TUNEL-positive nuclei was significantly increased (~30%) in the intestinal polyps of $Apc^{Min/+}$ mice following the loss of one allele of c-*myc* when compared with $Apc^{Min/+}$ c-$myc^{+/+}$ mice (~5%; Fig. 4D-F).

Having observed significant changes in levels of cell proliferation and apoptosis between $Apc^{Min/+}$ c-$myc^{+/+}$ and $Apc^{Min/+}$ c-$myc^{+/-}$ polyps, we chose to delve deeper into the cause of these changes. It has been shown that c-Myc can affect cell cycle progression by modulating the expression of cyclins or by altering cyclin activity, specifically cyclin D1 and cyclin E. Cyclins, along with cyclin-dependent kinases, are critical for G_1-S transition during cell cycle progression. It has been shown that *c-myc* is capable of directly inducing cyclin E expression as well as affecting cyclin E activity (23). Therefore, we examined expression of *cyclin D1* and *cyclin E* in normal intestinal tissue as well as in polyps of different sizes from animals that were either $Apc^{Min/+}$ c-$myc^{+/+}$ or $Apc^{Min/+}$ c-$myc^{+/-}$ by real-time PCR (Fig. 5B and C). We also examined the different-sized polyps for changes in c-*myc* expression, as amplification or overexpression of oncogenes is common in many cancers due to selective pressure (Fig. 5A). Examination of *cyclin D1* levels in normal intestinal tissue as well as in intestinal polyps of equal size displayed no difference in expression levels regardless of c-Myc status (Fig. 5B). Although surprising, these results were not entirely unexpected, as *cyclin D1* is also a direct β-catenin target gene (8). In addition, we examined c-*myc* and *cyclin E* expression (Fig. 5A and C). Although c-*myc* expression was significantly reduced in normal intestinal tissue in $Apc^{Min/+}$ c-$myc^{+/-}$ mice, as well as in polyps of equal sizes, there was a marked increase in c-*myc* expression in the larger polyps of $Apc^{Min/+}$ c-$myc^{+/-}$ mice (Fig. 5A). Moreover, the pattern of *cyclin E* expression seemed to correlate with the observed changes in c-*myc* expression in the different-sized polyps (Fig. 5A and C). Taken together, these data suggest that Myc is controlling cell cycle traverse through regulation of cyclin E levels and/or cyclin E activity.

Reduction in c-Myc Levels Correlates with a Decrease in the Expression of Angiogenic Factors

c-Myc has been shown to act as a master regulator of angiogenesis as well as apoptosis and cell cycle traverse (10, 14). Dysregulation of any of these processes could be the reason for the overall decrease in polyp numbers that we observed in $Apc^{Min/+}$ c-$myc^{+/-}$ animals (Fig. 2A, B, and D). Indeed, we observed a decrease in the levels of proliferation in intestinal polyps from $Apc^{Min/+}$ mice that were heterozygous for c-*myc* when compared with mice that were WT for c-*myc* (Fig. 3A and B). In addition, we also observed an increase in apoptosis in the polyps of $Apc^{Min/+}$ animals that were heterozygous for c-*myc* (Fig. 4D-F). It is doubtful that these modest changes in proliferation or apoptosis could account for the dramatic increases in survival or decreases in polyp size and number that we observed. This reasoning is based on our previous studies examining c-*myc* loss on teratoma formation in nude mice (14). Whereas c-*myc* loss had no significant effect on

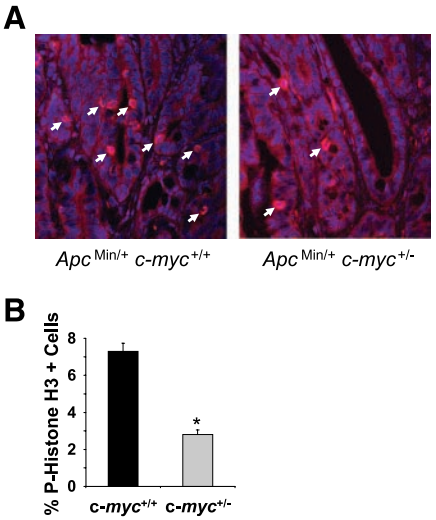

FIGURE 3. Cell proliferation is reduced in intestinal polyps of $Apc^{Min/+}$ c-$myc^{+/-}$ animals. **A.** Immunofluorescent images showing phospho-histone H3 (*P-Histone H3*)-positive cells (*red*) in intestinal polyps from WT (*left*) or c-$myc^{+/-}$ animals (*right*) that are $Apc^{Min/+}$. Sections were counterstained with 4′,6-diamidino-2-phenylindole (*blue*) to visualize nuclei. **B.** Cell proliferation is reduced in intestinal polyps present in $Apc^{Min/+}$ c-$myc^{+/-}$ mice. Graph showing the percentage of cells undergoing proliferation in $Apc^{Min/+}$ c-$myc^{+/+}$ (*black columns*) or $Apc^{Min/+}$ c-$myc^{+/-}$ (*gray columns*) mice. Data were obtained from z-series confocal sections (n = 10) of multiple intestinal tumors (n = 5) from multiple mice (n = 5 per group) and quantified using Image-Pro Plus software.

proliferation or apoptosis in embryonic stem cells, tumor formation was markedly reduced due to dysregulation of angiogenic factors (14). Thus, we next examined the expression of *VEGF* as well as several other factors involved in angiogenesis, including Eph receptor tyrosine kinases, which are deregulated in many human cancers, and their respective ligands, the ephrins (24, 25). We first examined the expression of VEGF in the whole animal using serum isolated from retro-orbital eye bleeds. Using serum isolated from WT, $Apc^{Min/+}$ c-$myc^{+/+}$, $Apc^{+/+}$ c-$myc^{+/-}$, or $Apc^{Min/+}$ c-$myc^{+/-}$ age-matched animals (8 weeks), we examined VEGF expression by ELISA (Fig. 6A). Loss of a single allele of c-*myc* resulted in a decrease in circulating VEGF in $Apc^{Min/+}$ mice when compared with $Apc^{Min/+}$ mice that were WT for c-*myc* (Fig. 6A). In the absence of the $Apc^{Min/+}$ mutation, c-*myc* loss displayed no effect on circulating VEGF protein levels (Fig. 6A). We next did real-time PCR analyses on normal intestinal tissue or intestinal polyps isolated from $Apc^{Min/+}$ mice that were WT or heterozygous for c-*myc* (Fig. 6B). These real-time PCR analyses showed marked decreases in the expression of *VEGF* in polyps isolated from c-$myc^{+/-}$ animals when compared with polyps isolated from animals that were WT for c-*myc* (Fig. 6B). Having observed increases in c-*myc* expression correlating with polyp size, we decided to examine *VEGF* expression in polyps of equal size (Fig. 6C). In the polyps that were WT for c-*myc*, we observed a large increase in the levels of *VEGF*, going from 2-fold over normal to >7-fold over normal levels in the largest polyps (Fig. 6C). Increases were also observed in the polyps that were heterozygous for c-*myc*, although the overall levels were not as high as those observed in the WT polyps (Fig. 6C). Furthermore, in addition to the marked decrease in *VEGF* expression, we also observed significant differences in *EphA2* and *ephrin-B2* expression when comparing WT polyps with c-$myc^{+/-}$ polyps (Fig. 6D). However, no differences in expression were observed for *EphB4* or *ephrin-A1* (Fig. 6D). Taken together, these data further support our hypothesis that c-Myc functions as a master regulator of cytokines, such as VEGF, to regulate cell growth, proliferation, and angiogenesis, and when c-Myc expression is deregulated or amplified, this leads to cancer.

Reduction in c-Myc Levels Restores Spleen Size and Hematocrit in $Apc^{Min/+}$ Animals

It has been well documented that $Apc^{Min/+}$ mice display splenomegaly and a decreased hematocrit when compared with

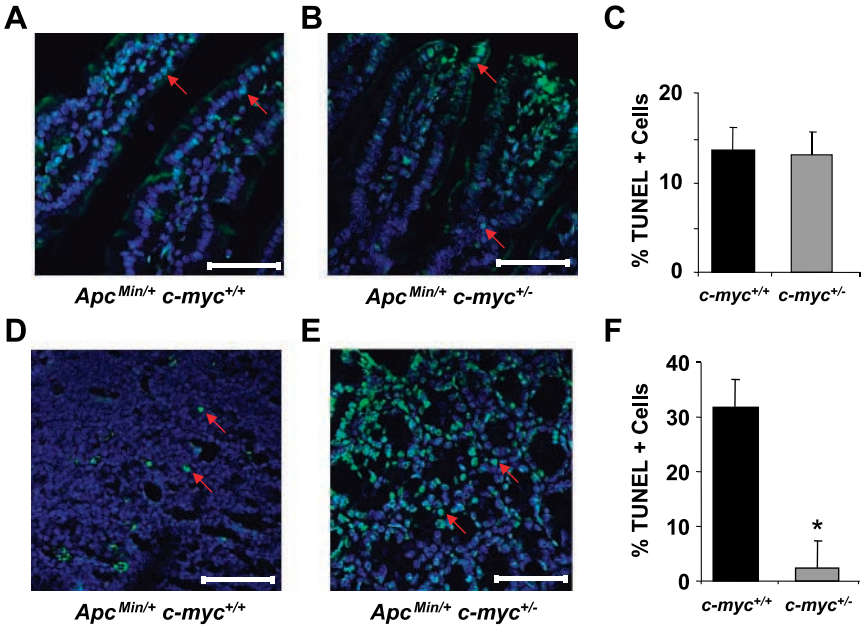

FIGURE 4. Effect of *c-myc* haploinsufficiency on apoptosis in the normal intestinal crypts and polyps of $Apc^{Min/+}$ mice. **A, B, D,** and **E.** TUNEL-positive nuclei were quantified in the normal intestinal crypts or polyps of WT (*black columns*) or c-$myc^{+/-}$ (*gray columns*) mice and expressed as percentage of total number of nuclei counted using Image-Pro Plus software in the representative ×40 confocal images. There is no significant difference in the percentage of TUNEL-positive nuclei in the normal intestinal crypts between $Apc^{Min/+}$ c-$myc^{+/+}$ and $Apc^{Min/+}$ c-$myc^{+/-}$ (**C**), but the percentage of TUNEL-positive nuclei is dramatically increased with loss of one allele of c-*myc* in polyps isolated from $Apc^{Min/+}$ intestines (**F**). n = 5 mice for each group; n = 5 crypts or polyps from each mouse. Bar, 50 μm.

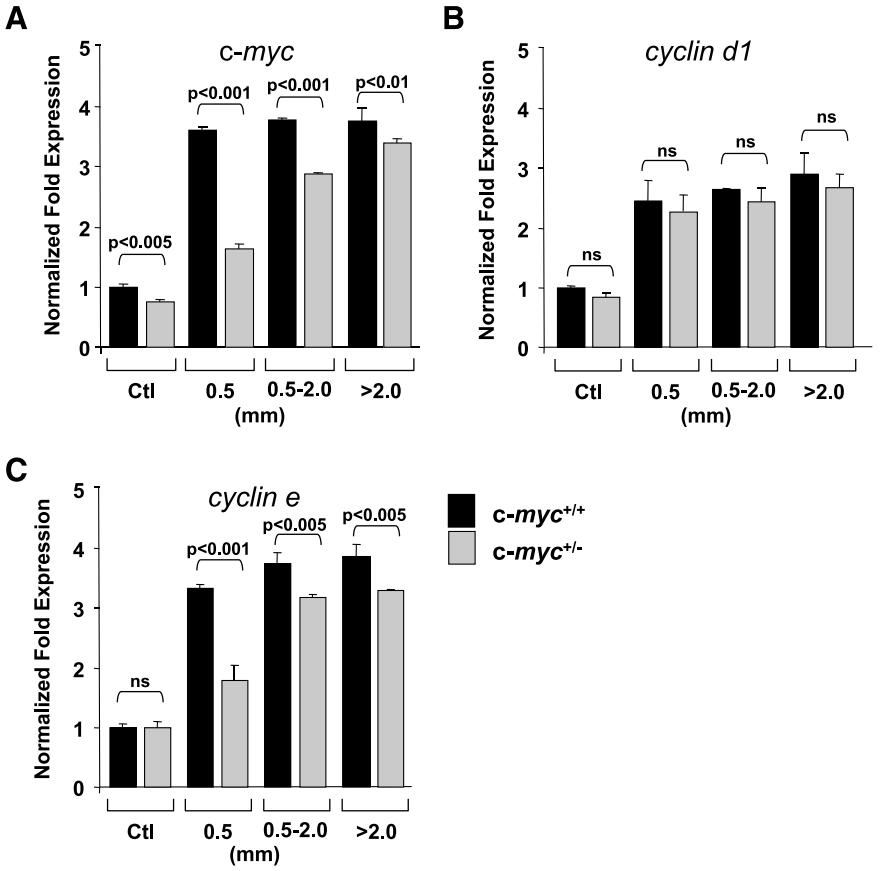

FIGURE 5. c-*myc* and *cyclin E*, but not *cyclin D1*, expression is increased in the intestinal polyps of $Apc^{Min/+}$ mice. **A.** Normal intestinal tissue or polyps of equal sizes (0.5 mm, 0.5-2.0 mm, or >2.0 mm) were examined for c-*myc* expression by real-time PCR. All samples are normalized to *ARPP P0* and then expression is plotted as fold of normal WT or c-$myc^{+/-}$ tissue. c-*myc* expression is reduced in $Apc^{Min/+}$ c-$myc^{+/-}$ (*gray columns*) when compared with $Apc^{Min/+}$ mice that are WT for c-*myc* (*black columns*). However, in the larger polyps, c-*myc* expression is amplified. **B.** *Cyclin D1* expression is unchanged regardless of c-*myc* expression. **C.** *Cyclin E* expression is reduced in intestinal polyps that are heterozygous for c-*myc*. Notice that the reduction in *cyclin E* expression correlates with levels of c-*myc* expression. Statistical significance between samples as determined by Student's *t* test ($n = 4$).

WT animals. Therefore, we examined the effect that c-*myc* loss had on spleen size and hematocrit, as well as examining WBC counts in the animals used in this study (12 weeks). Although we observed no detectable differences in the hematocrit levels of animals that were WT or heterozygous for c-*myc* in the absence of the $Apc^{Min/+}$ mutation, animals that were $Apc^{Min/+}$ c-$myc^{+/+}$ displayed a significantly reduced hematocrit (Fig. 7A). However, loss of one allele of c-*myc* in animals that were $Apc^{Min/+}$ returned their hematocrit levels to normal (Fig. 7A). Moreover, WBC counts were also normal in $Apc^{Min/+}$ c-$myc^{+/-}$ mice, whereas $Apc^{Min/+}$ mice that were WT for c-*myc* displayed WBC counts that were ~2-fold greater than those observed in WT animals (Fig. 7B). Finally, mice that were $Apc^{Min/+}$ c-$myc^{+/+}$ displayed enlarged spleens, with an average weight of ~260 mg, whereas $Apc^{Min/+}$ mice that were c-$myc^{+/-}$ displayed normal-sized spleens (~75 mg; Fig. 7C). These data clearly show that loss of only a single c-*myc* allele can restore hematocrit levels in $Apc^{Min/+}$ mice and protect these animals from tumorigenesis and the observed corresponding splenomegaly.

Discussion

The aim of this study was to evaluate the importance of the oncogene c-Myc in Apc-mediated intestinal tumorigenesis using the $Apc^{Min/+}$ mouse as a model. The *Apc* gene is defective in most colorectal cancers, including both inherited and sporadic forms, but the mechanisms through which Apc regulates tumorigenesis remain poorly understood. It has been previously shown that Apc normally controls cytosolic levels of β-catenin by proteasome degradation, preventing formation of the β-catenin/T-cell factor-4 complex and effectively blocking β-catenin/T-cell factor-4–meditated transcription (5). One of the downstream targets for β-catenin that has been identified is c-*myc* (7, 8). Indeed, previous studies have shown that the c-*myc* promoter is repressed by Apc in human colorectal cancer cells and c-*myc* expression is increased by overexpression of β-catenin (7). Thus, it seems that mutation of *Apc* leads to an increase in β-catenin activity and this leads to an increase in c-Myc expression and subsequently an increase in the expression of c-Myc target genes. Indeed, recent data from Sansom et al. (22) further support this through demonstration that c-Myc is required for activation of Wnt pathway target genes following *Apc* loss.

Myc activates or represses the transcription of a wide array of genes, including proangiogenic and antiangiogenic factors (14-16). Indeed, Myc overexpression in various cell types in mice induces tumors that display increased proliferation, delayed differentiation, and increased angiogenesis (16, 20). To better understand the role that c-Myc plays in Apc-mediated tumorigenesis, we examined tumor formation and survival in $Apc^{Min/+}$ animals that were either WT or heterozygous for c-*myc*. Our results clearly showed that c-Myc is critical for Apc-mediated tumorigenesis, as loss of a single allele of c-*myc* resulted in a dramatic increase in survival (Fig. 1). Additionally,

c-$myc^{+/-}$ animals displayed markedly fewer overall polyps than their WT littermates, as well as showing dramatic decreases in the number of larger polyps (>2.0 mm; 90% decrease; Fig. 2A and B). Surprisingly, we only observed a 2-fold change in the level of proliferation within the intestinal polyps following the loss of a single c-*myc* allele (Fig. 3A and B). We also examined the normal intestinal crypts as well as polyps for apoptosis. We observed no differences in the apoptotic indices in the normal intestinal crypts between WT and c-*myc* heterozygotes in $Apc^{Min/+}$ mice (Fig. 4A-C). However, the number of TUNEL-positive cells was significantly increased in adenomatous polyps in animals that were heterozygous for c-*myc* (Fig. 4D-F). These results are interesting, as previous studies from Alan Clarke's laboratory showed that there is a decrease in levels of apoptosis in the small intestine following loss of both *Apc* and c-*myc* in the adult animal (22). Furthermore, previous studies from our laboratory and others showed that c-*myc* loss has no effect on levels of apoptosis either in E9.5 embryos (14) or in the normal intestinal epithelium (13).

These effects on proliferation and apoptosis are due to changes in c-*myc* expression in the polyps of $Apc^{Min/+}$ mice. Indeed, when we examined c-*myc* expression in intestinal polyps from $Apc^{Min/+}$ c-$myc^{+/-}$ mice, we observed a significant decrease in c-*myc* expression in the smaller polyps when compared with those isolated from $Apc^{Min/+}$ mice that are WT for c-*myc* (Fig. 5A). However, in the larger polyps, the difference in c-*myc* expression is not as great (Fig. 5A). This increase in c-*myc* expression that is observed in the larger polyps of the $Apc^{Min/+}$ c-$myc^{+/-}$ mice could be due to loss of the WT *Apc* allele or could also be due to increases in c-Myc expression due to the hypoxic environment of the larger polyps. Indeed, several recent articles have shown that hypoxia can increase c-Myc expression and/or transcriptional activity (26, 27).

In addition to the observed proliferative and apoptotic changes in the $Apc^{Min/+}$ c-$myc^{+/-}$ mice, the polyps that did form in these animals ($Apc^{Min/+}$ c-$myc^{+/-}$) showed marked decreases in vascularization when compared with $Apc^{Min/+}$ c-$myc^{+/+}$ mice and the blood vessels present in the polyps from $Apc^{Min/+}$ c-$myc^{+/-}$ animals seem to be nonfunctional (data not shown). Finally, these decreases in vascularization seem to be due to significant reductions in levels of *VEGF, EphA2*, and *ephrin-B2* expression (Fig. 6B-D). Taken together, these studies show that c-Myc is an important downstream target of β-catenin and that c-Myc functions as an

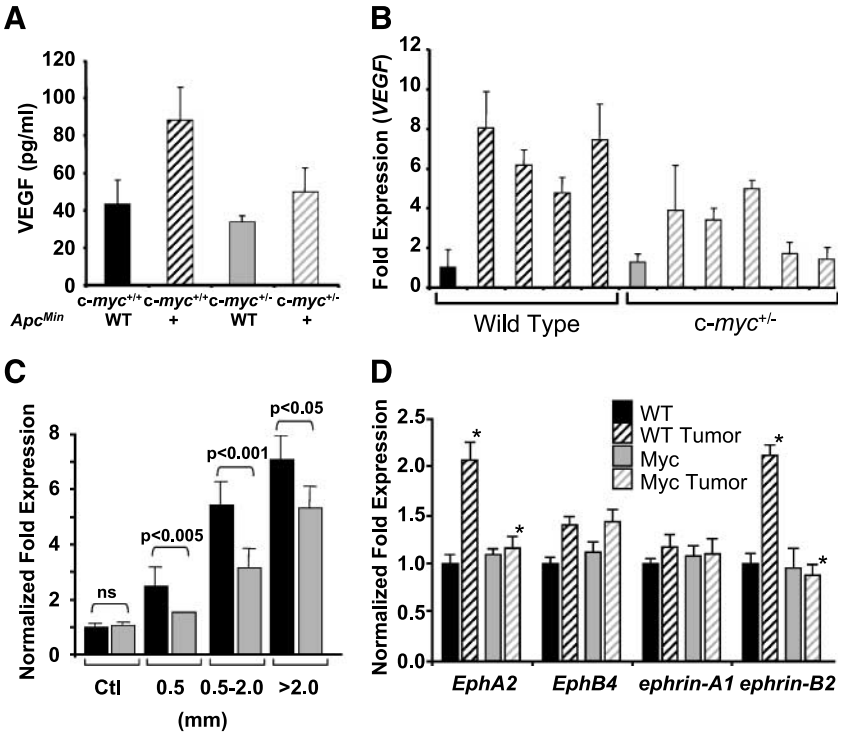

FIGURE 6. Reduced levels of c-*myc* result in decreased expression of angiogenic factors in tumors in the small intestine. **A.** Levels of VEGF present in the serum of age-matched (8 wk) WT (*solid black columns*), c-$myc^{+/-}$ (*solid gray columns*), or $Apc^{Min/+}$ mice that were either WT for c-*myc* (*black hatched columns*) or heterozygous for c-*myc* (*gray hatched columns*) are shown. Notice the increase in VEGF levels in $Apc^{Min/+}$ mice that are WT for c-*myc* ($n = 5$ per group). **B.** Normal intestinal tissue or intestinal polyps were examined for *VEGF* expression by real-time PCR. Total RNA was isolated from normal intestinal tissue from $Apc^{Min/+}$ c-$myc^{+/+}$ (*solid black columns*) or pooled intestinal polyps (*black hatched columns*) or normal tissue from $Apc^{Min/+}$ mice that were heterozygous for c-*myc* (*solid gray columns*) or pooled intestinal polyps (*gray hatched columns*). All samples were normalized to *ARPP P0* and then expression was plotted as fold of normal WT tissue. Significance between samples as determined by Student's *t* test ($n = 5$). **C.** Normal intestinal tissue or polyps of equal sizes (0.5 mm, 0.5-2.0 mm, or >2.0 mm) were examined for *VEGF* expression by real-time PCR. Notice that *VEGF* expression is reduced in $Apc^{Min/+}$ c-$myc^{+/-}$ (*gray columns*) when compared with $Apc^{Min/+}$ mice that are WT for c-*myc* (*black columns*). However, in the larger polyps, *VEGF* expression is increased, similar to that pattern observed for c-*myc* expression. Statistical significance between samples as determined by Student's *t* test ($n = 4$). **D.** Expression of several *Ephs* and *ephrins* in normal intestinal tissue and polyps. Total RNA was isolated and examined for *EphA2, EphB4, ephrin-A1*, and *ephrin-B2* expression. As in **B**, all samples were normalized to *ARPP P0*. c-*myc* expression only alters the expression of *EphA2* and *ephrin-B2*. Asterisks, significance between the sample and all other samples as determined by Student's *t* test ($n = 5$).

important mediator of polyp growth and colorectal cancer initiation by regulating factors that are essential for angiogenesis to allow for adequate vascularization, supply of nutrients, and tumorigenesis. These studies further strengthen the importance of c-Myc as a target for novel therapeutic modalities in the treatment of colorectal cancers as well as other cancers with deregulated Myc expression.

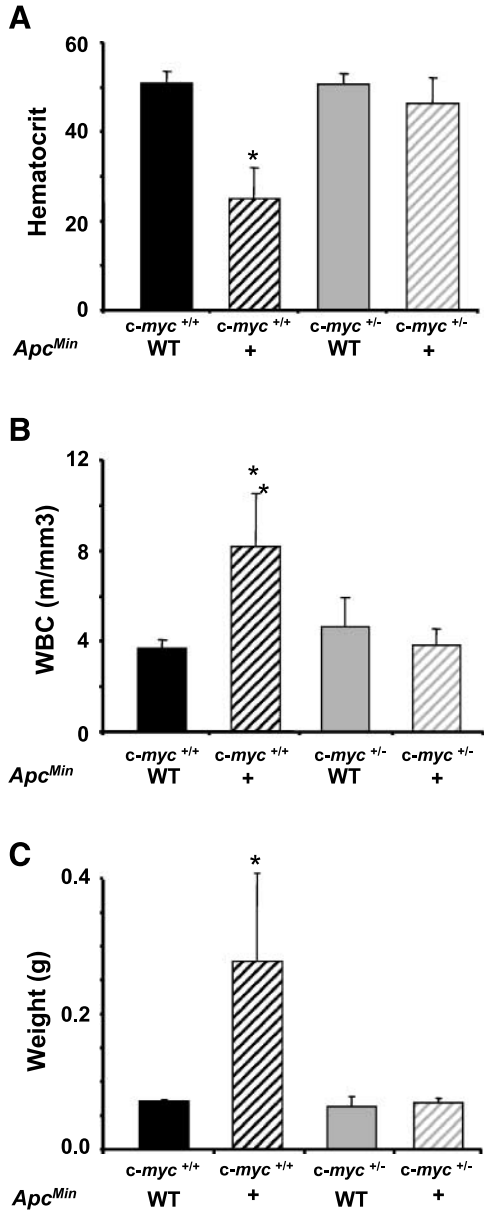

FIGURE 7. Reduced c-*myc* expression in $Apc^{Min/+}$ mice restores spleen size and a normal hematocrit. **A.** Blood was isolated from age-matched animals (12 wk) that were either $Apc^{+/+}$ c-$myc^{+/+}$, $Apc^{Min/+}$ c-$myc^{+/+}$, $Apc^{+/+}$ c-$myc^{+/-}$, or $Apc^{Min/+}$ c-$myc^{+/-}$ and hematocrit was determined. **B.** WBC counts were restored in $Apc^{Min/+}$ mice on c-*myc* loss. **C.** Loss of c-*myc* eliminated splenomegaly in $Apc^{Min/+}$ mice. Following eye bleeds, hematocrit and WBC counts were done using a VetScan HM2 Hematology System. Following blood isolation, animals were humanely sacrificed and spleens were isolated and weighed. Asterisks, significance between the sample and all other samples as determined by Student's *t* test ($n = 5$).

Materials and Methods

Animal Studies

$Apc^{Min/+}$ mice on a pure C57BL/6 background were mated to c-$myc^{+/-}$ mice on a mixed C57BL/6 × SV129 background, and the resulting pups were screened for the Min mutation (28) and for the c-*myc*−null gene (14) by PCR as previously described. Animals that were homozygous for the WT *c-myc* gene and heterozygous for the Min mutation served as controls. Animals were housed and bred within the Animal Resources Facility at the University of South Carolina School of Medicine. Primer sequences for genotyping are available on request.

Polyp Number Determination

Intestinal adenomas and colonic adenomas were scored for numbers and size (diameter) at postnatal day 84 (age matched) or when the animal was moribund. The mice were weighed and sacrificed by cervical dislocation and blood and serum were obtained. In addition, the small and large intestines and colon were isolated. The intestinal tract was rinsed with cold PBS using a blunt-end syringe and opened along the longitudinal axis. The opened intestine was spread flat between sheets of filter paper and fixed in fresh 4% paraformaldehyde. Paraformaldehyde-fixed intestinal sections were rinsed in deionized water and stained with 0.2% methylene blue and polyps were counted at ×20 magnification under a dissecting microscope using tweezers to pick through the intestinal villi and identify polyps. Polyps were categorized as >0.5 mm, 0.5 to 2.0 mm, or >2.0 mm in size. After polyps were counted, intestinal sections were placed in 70% ethanol for further analysis. For each experimental group, the incidence of tumors, defined as the number of mice with tumors/number of mice in the group, the mean number of tumors/mouse ± SD, and the mean tumor diameter (mm) in the group ± SD were calculated for the intestine and colon separately. Student's *t* test was used to compare means of each group; differences were considered to be significant if P values were <0.05. For histology, segments of intestine and colon were paraffin embedded; 5-μm sections were cut and stained with H&E. In addition, whole mount images were taken at ×20 to show differences in polyp size and number.

Measurement of Hematocrit and Spleen Weight

For measurement of hematocrit and WBC counts, retro-orbital eye bleeds (200 μL) were done on WT, $Apc^{Min/+}$ c-$myc^{+/+}$, $Apc^{+/+}$ c-$myc^{+/-}$, and $Apc^{Min/+}$ c-$myc^{+/-}$ age-matched animals (12 weeks) and samples were analyzed using the VetScan HM2 Hematology System (Abaxis). Animals were then sacrificed and their spleens were isolated and weighed ($n = 5$). In addition, their small and large intestines and colon were isolated as described above for further analyses.

ELISA Measurement of VEGF

Retro-orbital bleeds were done as described above on age-matched animals (8 weeks) and blood samples were allowed to coagulate and samples were centrifuged at 14,000 × *g* for 10 min to isolate blood serum. Serum was then assayed for VEGF protein levels using an ELISA assay specific for murine VEGF as described by the manufacturer (R&D Systems).

Real-time PCR Analyses

Total RNA was isolated from normal intestinal tissue or intestinal tumor tissue using Trizol reagent (Invitrogen) as described by the manufacturer. Real-time PCR analyses were done using a Bio-Rad reverse transcription-PCR kit for probes and the Bio-Rad iQ5 Real-time Thermocycler (Bio-Rad) as described by the manufacturer. We used primer/probe sets that were specific for murine *c-myc, cyclin D1, cyclin E, VEGF, EphA2, EphB4, ephrin-A1, ephrin-B2*, and *ARPP P0. ARPP P0* served as our internal control for normalization. Primer and probe sequences are available on request.

Tissue Isolation and Cell Proliferation Analyses

Immunofluorescent analyses were done on intestines isolated from 12-week-old $Apc^{Min/+}$ c-$myc^{+/+}$ and $Apc^{Min/+}$ c-$myc^{+/-}$ animals. Briefly, intestines were fixed in fresh 4% paraformaldehyde overnight at 4°C and 120-μm-thick sections were cut using a vibratome (Oxford Instruments). Sections were permeabilized using PBS containing 0.01 mol/L glycine and 0.1% Triton X-100 for 1 h at room temperature. The sections were then blocked using PBS containing 5% bovine serum albumin for 1 h at room temperature. Antibody against phosphohistone H3 (Santa Cruz Biotechnology) was used at a 1:200 concentration. Sections were incubated with primary antibody in 1% blocking buffer (1% bovine serum albumin/PBS) overnight at 4°C. Sections were washed and incubated with donkey anti-rabbit FITC secondary antibody (Zymed) at a 1:100 concentration in 1% blocking buffer for 2 h at room temperature. In addition, sections were stained with Texas red phalloidin for actin visualization and nuclei were visualized through staining with 4′,6-diamidino-2-phenylindole (Molecular Probes). Intestinal sections were imaged using a Leica LSM 510 laser scanning microscope. Image-Pro Plus software was used to quantify total number of nuclei and nuclei that were phosphohistone H3 positive per representative ×40 high magnification field. Five polyps were analyzed from five individual mice for each genotype ($Apc^{Min/+}$ c-$myc^{+/+}$ and $Apc^{Min/+}$ c-$myc^{+/-}$).

Cell Death Detection In situ *Using TUNEL*

Apoptotic cells in the intestinal polyps were visualized using the TUNEL method (Roche Molecular Biochemicals) as described by the manufacturer. Briefly, deparaffinized tissue sections were permeabilized using Triton X-100 (Sigma). The sections were then incubated with TUNEL reaction mixture containing terminal deoxynucleotidyl transferase and fluorescein-dUTP, at 37°C for 30 min, rinsed in PBS for 10 min, mounted, and analyzed using a Leica LSM 510 laser scanning microscope. Image-Pro Plus software was used to quantify the number of TUNEL-positive nuclei. DNase I–treated tissue sections were used as positive controls. TUNEL-positive nuclei were expressed as percent of total number of nuclei counted per representative ×40 higher magnification image. Scale bars are set at 50 μm.

Acknowledgments

We thank Drs. Frank Berger and Tom Borg for their mentorship and valuable comments and Arti Intwala for her work in breeding, maintaining, and genotyping our mouse colonies.

References

1. Smith KJ, Johnson KA, Bryan TM, et al. The APC gene product in normal and tumor cells. Proc Natl Acad Sci U S A 1993;90:2846–50.

2. Groden J, Thliveris A, Samowitz W, et al. Identification and characterization of the familial adenomatous polyposis coli gene. Cell 1991;66:589–600.

3. Kinzler KW, Nilbert MC, Su LK, et al. Identification of FAP locus genes from chromosome 5q21. Science 1991;253:661–5.

4. Nishisho I, Nakamura Y, Miyoshi Y, et al. Mutations of chromosome 5q21 genes in FAP and colorectal cancer patients. Science 1991;253:665–9.

5. Morin PJ, Sparks AB, Korinek V, et al. Activation of β-catenin-Tcf signaling in colon cancer by mutations in β-catenin or APC. Science 1997;275:1787–90.

6. Korinek V, Barker N, Moerer P, et al. Depletion of epithelial stem-cell compartments in the small intestine of mice lacking Tcf-4. Nat Genet 1998;19:379–83.

7. He TC, Sparks AB, Rago C, et al. Identification of c-MYC as a target of the APC pathway. Science 1998;281:1509–12.

8. Tetsu O, McCormick F. β-Catenin regulates expression of cyclin D1 in colon carcinoma cells. Nature 1999;398:422–6.

9. Barker N, Morin PJ, Clevers H. The yin-yang of TCF/β-catenin signaling. Adv Cancer Res 2000;77:1–24.

10. Eisenman RN. Deconstructing myc. Genes Dev 2001;15:2023–30.

11. Grandori C, Cowley SM, James LP, Eisenman RN. The Myc/Max/Mad network and the transcriptional control of cell behavior. Annu Rev Cell Dev Biol 2000;16:653–99.

12. Pelengaris S, Khan M, Evan G. c-MYC: more than just a matter of life and death. Nat Rev Cancer 2002;2:764–76.

13. Bettess MD, Dubois N, Murphy MJ, et al. c-Myc is required for formation of intestinal crypts but dispensable for homeostasis of the adult intestinal epithelium. Mol Cell Biol 2005;25:7868–78.

14. Baudino TA, McKay C, Pendeville-Samain H, et al. c-Myc is essential for vasculogenesis and angiogenesis during development and tumor progression. Genes Dev 2002;16:2530–43.

15. Mezquita P, Parghi SS, Brandvold KA, Ruddell A. Myc regulates VEGF production in B cells by stimulating initiation of VEGF mRNA translation. Oncogene 2005;24:889–901.

16. Pelengaris S, Littlewood T, Khan M, Elia G, Evan G. Reversible activation of c-Myc in skin: induction of a complex neoplastic phenotype by a single oncogenic lesion. Mol Cell 1999;3:565–77.

17. Tikhonenko AT, Black DJ, Linial ML. Viral Myc oncoproteins in infected fibroblasts down-modulate thrombospondin-1, a possible tumor suppressor gene. J Biol Chem 1996;271:30741–7.

18. Watnick RS, Cheng YN, Rangarajan A, Ince TA, Weinberg RA. Ras modulates Myc activity to repress thrombospondin-1 expression and increase tumor angiogenesis. Cancer Cell 2003;3:219–31.

19. Nesbit CE, Tersak JM, Prochownik EV. MYC oncogenes and human neoplastic disease. Oncogene 1999;18:3004–16.

20. Ruddell A, Mezquita P, Brandvold KA, Farr A, Iritani BM. B lymphocyte-specific c-Myc expression stimulates early and functional expansion of the vasculature and lymphatics during lymphomagenesis. Am J Pathol 2003;163:2233–45.

21. Ignatenko NA, Holubec H, Besselsen DG, et al. Role of c-Myc in intestinal tumorigenesis of the ApcMin/+ mouse. Cancer Biol Ther 2006;5:1658–64.

22. Sansom OJ, Meniel VS, Muncan V, et al. Myc deletion rescues Apc deficiency in the small intestine. Nature 2007;446:676–9.

23. Deb-Basu D, Karlsson A, Li Q, Dang CV, Felsher DW. MYC can enforce cell cycle transit from G_1 to S and G_2 to S, but not mitotic cellular division, independent of p27-mediated inhibition of cyclin E/CDK2. Cell Cycle 2006;5:1348–55.

24. Surawska H, Ma PC, Salgia R. The role of ephrins and Eph receptors in cancer. Cytokine Growth Factor Rev 2004;15:419–33.

25. Brantley-Sieders D, Parker M, Chen J. Eph receptor tyrosine kinases in tumor and tumor microenvironment. Curr Pharm Des 2004;10:3431–42.

26. Gordon JD, Bertout JA, Hu CJ, Diehl JA, Simon MC. HIF-2α promotes hypoxic cell proliferation by enhancing c-myc transcriptional activity. Cancer Cell 2007;11:335–47.

27. Liu J, Narasimhan P, Lee YS, et al. Mild hypoxia promotes survival and proliferation of SOD2-deficient astrocytes via c-Myc activation. J Neurosci 2006;26:4329–37.

28. Moser AR, Pitot HC, Dove WF. A dominant mutation that predisposes to multiple intestinal neoplasia in the mouse. Science 1990;247:322–4.